

Fig.6 Vector control scheme for DFIG

Two voltage-fed PWM converters are inserted in the rotor circuit, with the supply-side PWM converter connected to the stator/supply via three single-phase chokes. The voltage-transfer characteristics of the system, including the three phase back-to-back PWM converters, are given approximately by:

$$\begin{aligned} V_s &= m_1 \frac{\sqrt{3}E}{2\sqrt{2}} \\ V_r &= \pm s \frac{V_s}{n} = m_2 \frac{E}{2\sqrt{2}} \\ s &= \pm \frac{nm_2}{\sqrt{3}m_1} \end{aligned} \quad (3)$$

Where n is the stator-rotor turns ratio of the DFIG, s is the slip and m_1 , m_2 are the PWM modulation depths of the stator-side and rotor side converters respectively.

Eqn. (3) determines the speed range of the generator. For wind generation, a restricted speed range is acceptable on account of a minimum wind velocity (the cut-in speed), below which very little energy is extractable. The generator speed corresponding to rated wind velocity can be set at any point by the choice of gearbox ratio. Of course, to get the maximum benefit from the Scherbius scheme, this point should be well above synchronous speed where power is extracted from both the rotor and stator of the machine. Eventually, however, as the slip is increased, the system efficiency starts to decrease since more power passes through the DC link converters and the rotor iron and frictional losses increase.

A. Grid (Supply) Side Converter Control

The objective of the vector-control scheme for the grid-side PWM converter is to keep the DC-link voltage constant regardless of the magnitude and direction of the rotor power, while keeping sinusoidal grid currents. Decoupled control of active and reactive powers flowing between rotor and grid is done by using supply voltage vector oriented control (d^e-q^e). All voltage and current quantities are transformed to a special reference frame that rotates at the same speed as the supply voltage space phasor with the real axis (d -axis) of the reference frame aligned to the supply voltage vector. At steady state, the reference frame speed equals the synchronous speed. In such a scheme, current i_{gd}^e is controlled to keep the dc link voltage constant and current i_{gq}^e is used to obtain the

desired value of reactive power flow between the supply side converter and the supply. It may also be responsible for controlling reactive power flow between the grid and the grid side converter by adjusting $Q_{r,ref}$.

The scheme makes use of the supply voltage angle determined dynamically to map the supply voltage, the converter terminal voltage and the phase currents onto the new reference frame. First the supply voltage angle (θ) has to be determined.

By definition, the supply voltage angle is:

$$\theta = \tan^{-1} \left(\frac{V_{sq}^e}{V_{sd}^e} \right) \quad (4)$$

Aligning the d -axis of the reference frame along the supply-voltage position, $V_{sq}^e = 0$, and, since the amplitude of the supply voltage is constant V_{sd}^e is constant. The active and reactive power will be:

$$\begin{aligned} P_{gc} &= \frac{3}{2} (V_{sd}^e i_{gd}^e + V_{sq}^e i_{gq}^e) = \frac{3}{2} (V_{sd}^e i_{gd}^e) \\ Q_{gc} &= \frac{3}{2} (V_{sq}^e i_{gd}^e - V_{sd}^e i_{gq}^e) = -\frac{3}{2} (V_{sd}^e i_{gq}^e) \end{aligned} \quad (5)$$

The dc power has to be equal to the active power flowing between the grid and the grid side converter. Thus,

$$\begin{aligned} E i_{os} &= \frac{3}{2} (V_{sd}^e i_{gd}^e) \\ C \frac{\partial E}{\partial t} &= i_{os} - i_{or} \end{aligned} \quad (6)$$

Where, i_{os} is the current between the dc link and the stator and i_{or} is the current between the dc link and the rotor. Thus, the dc link voltage can be controlled by controlling i_{gd}^e .

The control scheme thus utilizes current control loops for i_{gd}^e and i_{gq}^e with the i_{gd}^e demand being derived from the DC-link voltage error through a standard PI controller as shown in Fig.7. The current i_{gq}^e reference was forced to zero so as to make the displacement equal to zero.

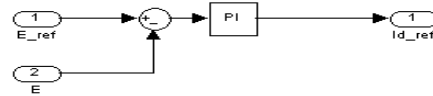


Fig.7. Reference current from DC link voltage error

B. Rotor-Side Converter Control

The vector-control scheme for the rotor-side PWM converter ensures decoupling control of stator-side active and reactive power drawn from the grid. To exploit the advantages of variable speed operation, the tracking of optimum torque-speed curve is essential. Speed can be adjusted to the desired value by controlling torque. So, an approach of using active power set point from the instantaneous value of rotor speed and controlling the rotor current i_{rd}^e in line voltage reference frame to get the desired active power will result in obtaining the desired values of speed and torque according to the optimum torque speed curve. The reference value of the stator-side active power is obtained via a look-up table for a given generator rotor speed, which enables the optimal power

tracking for maximum energy capture from the wind. Normally, the reference values of both stator-side and rotor side reactive power, Q_{sref} , Q_{rref} and are all set to zero to ensure unity power factor operation of the studied wind turbine.

Using the same approach like the grid side converter, the stator and rotor currents are transformed to the new reference frame using the voltage angle calculated in eqn. (4).

Stator flux linkage expressed in the new reference frame:

$$\begin{aligned}\lambda_{sd}^e &= L_s i_{sd}^e + L_m i_{rd}^e \\ \lambda_{sq}^e &= L_s i_{sq}^e + L_m i_{rq}^e\end{aligned}\quad (7)$$

Where, $L_s = L_{ls} + L_m$

Aligning the d -axis of reference frame to be along the line voltage will result in:

$\lambda_{sd}^e = 0$ and neglecting stator resistance will lead to $V_{sq} = 0$. Substituting for $V_{sq} = 0$, the active and reactive power will be simplified as follows:

$$\begin{aligned}P_s &= \frac{3}{2} (V_{sd}^e i_{sd}^e + V_{sq}^e i_{sq}^e) = \frac{3}{2} (V_{sd}^e i_{sd}^e) \\ Q_s &= \frac{3}{2} (V_{sq}^e i_{sd}^e - V_{sd}^e i_{sq}^e) = \frac{-3}{2} (V_{sd}^e i_{sq}^e)\end{aligned}\quad (8)$$

Therefore, the above equations show that active and reactive powers of the stator can be controlled independently.

From Eqn. 7,

$$\begin{aligned}\lambda_{sd}^e &= L_s i_{sd}^e + L_m i_{rd}^e = 0 \\ i_{sd}^e &= \frac{-L_m}{L_s} i_{rd}^e\end{aligned}\quad (9)$$

Substituting for i_{sd}^e into the torque and active power equation will result in:

$$P_s = \frac{3}{2} (V_{sd}^e i_{sd}^e) = -\frac{3}{2} \frac{L_m}{L_s} (V_{sd}^e i_{rd}^e)\quad (10)$$

The stator magnetizing current is

$$\vec{i}_{ms} \rightarrow = \frac{\lambda_{sd}^e + j\lambda_{sq}^e}{L_m}$$

$$\vec{i}_{ms} \rightarrow = \frac{j\lambda_{sq}^e}{L_m}$$

Thus, $\vec{i}_{ms} \rightarrow = |i_{ms}|$ is a constant value.

From Eqn. 7,

$$i_{sq}^e = \frac{\lambda_{sq}^e - L_m i_{rq}^e}{L_s} = \frac{L_m}{L_s} (|i_{ms}| - i_{rq}^e)\quad (11)$$

$$Q_s = \frac{-3}{2} (V_{sd}^e i_{sq}^e) = \frac{-3}{2} \frac{L_m}{L_s} V_{sd}^e (|i_{ms}| - i_{rq}^e)\quad (12)$$

Thus, the variations in rotor currents will also reflect in the variation of stator side currents, i_{sd}^e , i_{sq}^e and hence in the stator side real and reactive powers also. This principle has been used in the control of stator real and reactive powers.

The control scheme uses a PI controller to obtain the reference value for i_{rd}^e from real power error that is the difference between desired and actual values of real power. Similarly, a PI controller can be tuned to get the reference value for i_{rq}^e from the reactive power error. Then, both reference currents were transformed to their natural reference frame that is the rotor frame. These rotor current references, after a dq -to- abc transformation, were used for implementing the technique on the rotor side three-phase converter.

4. Results and Discussions

This study is made with simulation on the Matlab/Simulink and Power System Block Set modules. The induction machine is modelled on the stationary reference frame. With stationary reference frame, the speed of the reference frame is equal to zero. Stator and rotor voltage equation, flux linkage equation and torque equation are utilized for modelling in term of q component, d component and zero component. Stator and rotor circuits are assumed to be star connected. In addition, all rotor parameters are transformed to stator side via stator-rotor turns ratio (in this study a turn ratio of 1 is assumed).

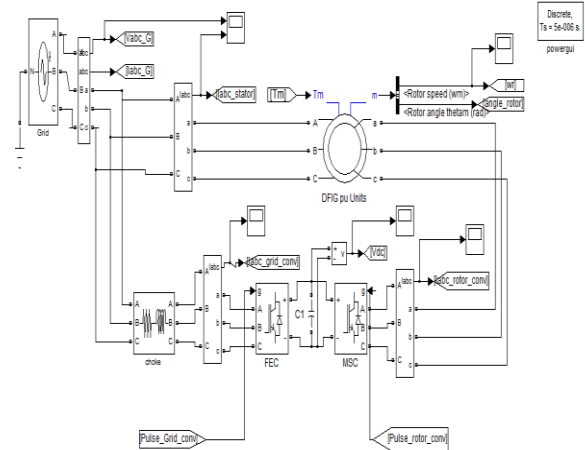


Fig.8 Simulink model of Grid connected DFIG

The tracking characteristic obtained through a look up table for different turbine speed ω_r by interpolation-extrapolation is shown Fig. 9.

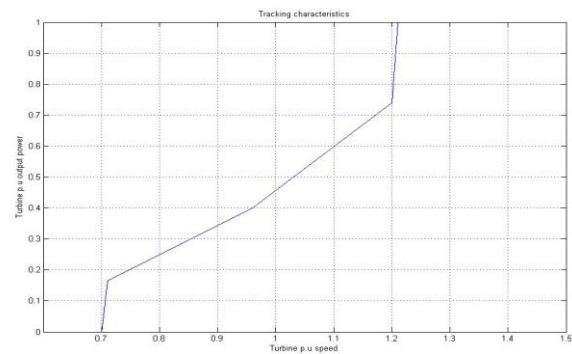


Fig. 9. Tracking characteristics

A. Sub-synchronous generation

Figures 10 to 17 show response of the system for such application. Fig. 10 shows that the measured active

power at the grid terminal and the reference active power from the optimal tracking are the same at steady state. Output Torque (T_m) from the wind turbine and reference active power (P_{sref}) from optimal power tracking is depicted in Fig. 11. The pitch angle is kept constant at its maximum value (zero) for sub-synchronous generation where the output power is below the rated value as shown in Fig. 12. The DC link voltage is held constant by the grid side converter controller as presented in Fig. 14. The measured reactive power and the reference reactive power are both zero at steady state as seen Fig. 15. The stator voltage and current are shown in Fig. 16.

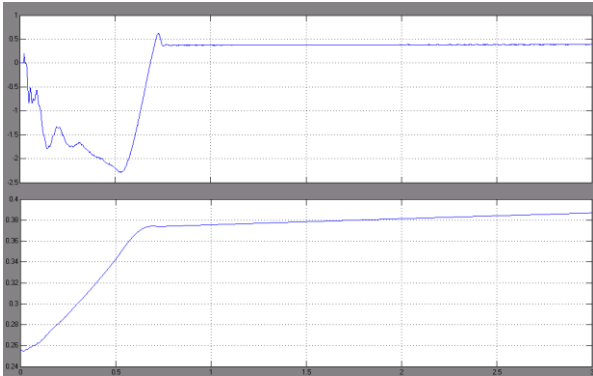


Fig. 10 Actual active power (P_s , upper) and reference active power (P_{sref} , lower)

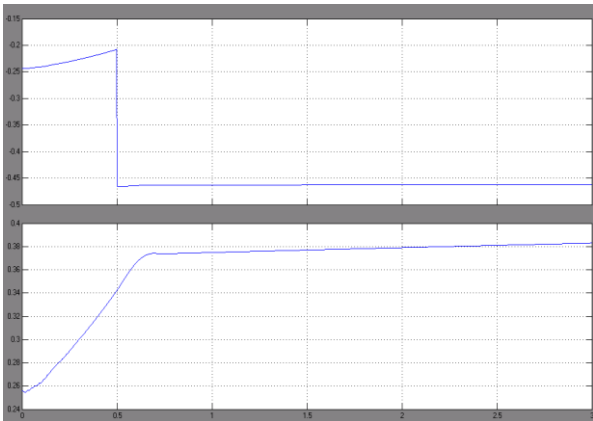


Fig. 11 Output Torque (T_m , upper) and reference active power (P_{sref} , lower)

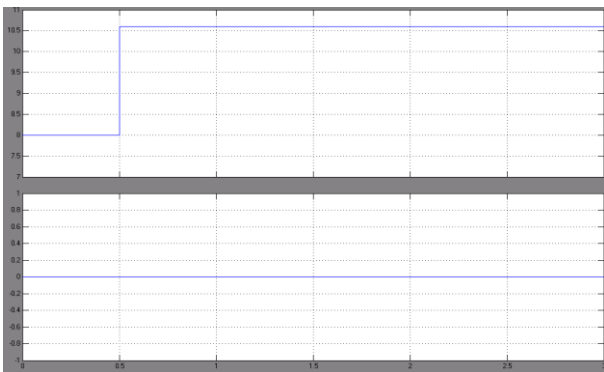


Fig. 13 Wind speed (upper) Vs pitch angle (lower)

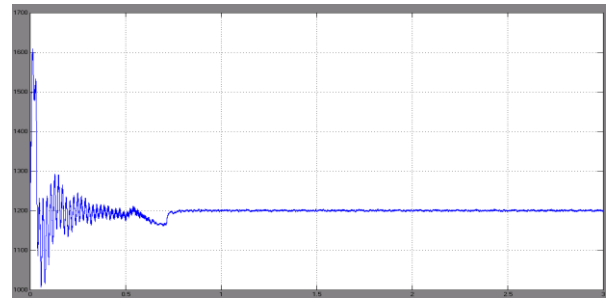


Fig. 14 DC link voltage

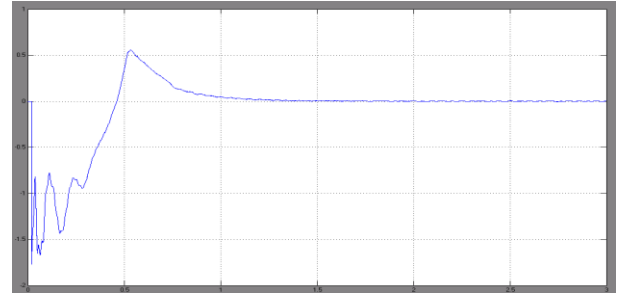


Fig. 15 Actual reactive power Q_s when reference reactive Power (Q_{sref}) is zero

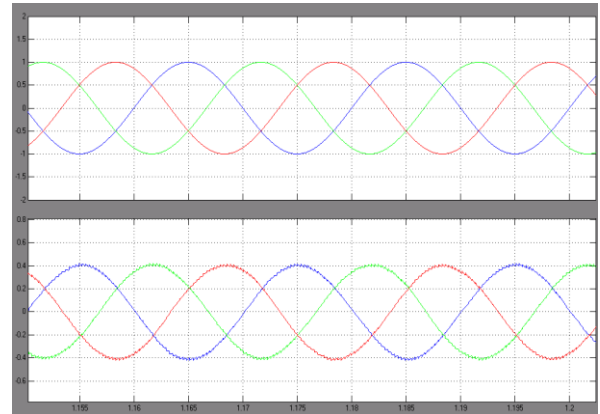


Fig.16. Stator voltage (upper) and current (lower)

B. Super-synchronous generation

Figure 17 and 18 show the response of the system for super-synchronous generation. As depicted in Fig. 17, the output torque is limited because the pitch angle is called in to action since from the tracking characteristics (Fig.9) the output power corresponding to the wind speed is above the rated value. Fig. 18 shows that the pitch angle control is called in to action when the generator speed is above 1.21 p.u. The pitch angle limits the output power and torque.

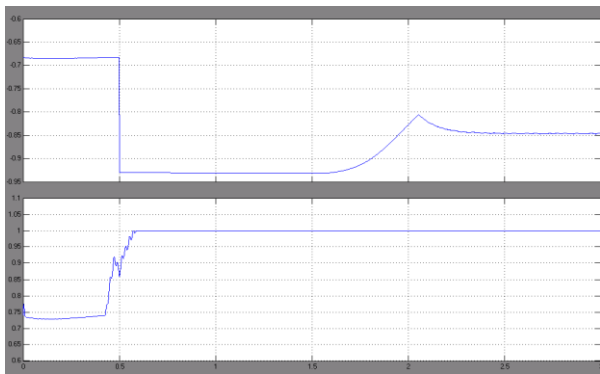


Fig. 17 Output torque (T_m , upper) and reference active power (P_{sref} , lower)

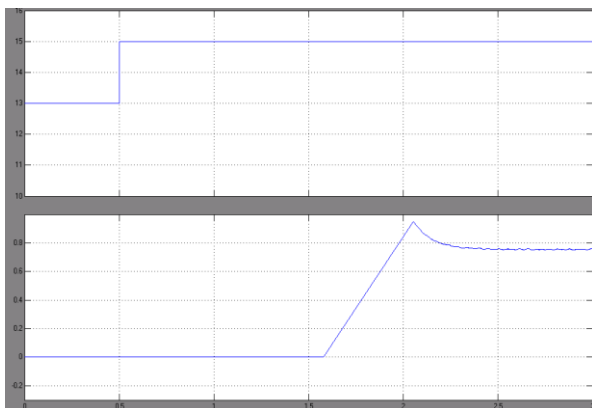


Fig. 18 Wind speed (upper) vs pitch angle (lower)

5. Conclusion

It is shown that a variable speed system using wound rotor induction machine controlled from the rotor side is superior because of higher energy output, lower rating (hence, lower cost) of converters, and better utilization of a generator when compared to systems using a cage rotor induction machine with the same rating. It has been shown from the simulation results that, using vector control, the reference active power from the wind and the measured active power at the grid terminals are equal both at sub-synchronous and super-synchronous speed operation. In order to limit the energy capture above the rated value pitch control has been implemented to the system and Simulation results show that the controller maintains the extracted energy till the rated value of the wind turbine mechanical power output.

Acknowledgment

The authors acknowledge the support provided by the Deanship of Scientific Research, King Fahd University of Petroleum & Minerals, through Electrical Power and Energy Systems Research Group funded project # RG1420-1&2.

References

- [1] <http://www.gwec.net/global-figures/graphs/>
- [2] Rajib Datta, V. T. Ranganathan "Variable-Speed Wind Power Generation Using Doubly Fed Wound Rotor Induction Machine—A Comparison with Alternative Schemes" IEEE Transactions on Energy Conversion, Vol. 17, No. 3, September 2002
- [3] Alan Mullane, Mark O'Malley "The Inertial Response of Induction- Machine- Based Wind Turbines" IEEE

- Transactions on Power Systems, Vol. 20, No. 3, August 2005
- [4] L. Cadirci, M. Ermiq "Double-output induction generator operating at Sub synchronous and super synchronous speeds: steady-state performance optimization and wind-energy recovery" IEE Proceedings-B, Vol. 139, No. 5, September 1992
- [5] Debiprasad Panda I, Thomas .A.Lipo "Double side control of wound rotor induction machine for wind energy application employing half controlled converters" IEEE Transactions on Energy Conversion, 2005
- [6] Debiprasad Panda, Eric L. Benedict, Giri Venkataramanan, Thomas A. Lipo" A Novel Control Strategy for the Rotor Side Control of a Doubly-Fed Induction Machine" 2001 IEEE
- [7] B. Rabelo, W. Hofmann, "Power Flow Optimization and Grid Integration of Wind Turbines with the Doubly-Fed Induction Generator" IEEE Transactions on Energy Conversion, 2005
- [8] Mohammad Jafar Zandzadeh, Abolfazl Vahedi, "Modeling and improvement of direct power control of DFIG under unbalanced grid voltage condition", Electrical Power and Energy Systems, 59, 58–65, 2014.
- [9] Muhammed Y. Worku, "Power Smoothing Control of PMSG Based Wind Generation Using Supercapacitor Energy Storage System", International Journal of Emerging Electric Power Systems. 2017; 20160181
- [10] Muhammed Y. Worku, M. A. Abido, and R. Iravani, " PMSG based wind system for real-time maximum power generation and low voltage ride through", Journal of Renewable Sustainable Energy 9, 013304 (2017); doi: 10.1063/1.4976141
- [11] P.W. Carlin, A.S. Laxson, E.B. Muljadi, "The History and State of the Art of Variable-Speed Wind Turbine Technology" National Renewable Energy Laboratory, February 2001
- [12] Muhammed Yibre and M. A. Abido, "Supercapacitors for wind power application", International Conference on Renewable Energy Research and Applications, Madrid, Spain, 20-23 October 2013.
- [13] Lihui Yang, Zhao Xu, Jacob ostergaard, Zhao Yang Dong, and Kit Po Wong, "Advanced Control Strategy of DFIG Wind Turbines for Power System Fault Ride Through", IEEE TRANSACTIONS ON POWER SYSTEMS, Vol. 27, No. 2, May 2012.
- [14] Andrew Miller, Edward Muljadi, Donald S. Zinger "A Variable Speed Wind Turbine Power Control" IEEE Transactions on Energy Conversion, Vol. 12, No.2, June 1997
- [15] Muhammed H. Rashid "Power Electronics Circuits, Devices, and Applications" Pearson Education, Third edition 2004
- [16] E. Muljadi, K. Pierce, P. Migliore" Control Strategy for Variable-Speed, Stall-Regulated Wind Turbines" Presented at American Controls Conference Philadelphia, PA June 24–26, 1998
- [17] E. Muljadi, C.P. Butterfield "Pitch-Controlled Variable-Speed Wind Turbine Generatio "Presented at the 1999 IEEE Industry Applications Society Annual Meeting Phoenix, Arizona October 3-7, 1999
- [18] Alexander Helmedag, Timo Isermann, and Antonello Monti, "Fault Ride Through Certification of Wind Turbines Based on a Hardware in the Loop Setup", IEEE Transactions on Instrumentation and Measurement, Vol. 63, No. 10, October 2014.
- [19] Tao Sun, Zhe Chen, Frede Blaabjerg, "Flicker Study on Variable Speed Wind Turbines with Doubly Fed Induction Generators" IEEE Transactions on Energy Conversion, Vol. 20, No. 4, December 2005.